

# Performance Analyses and Optimization of Real-time Multi-step GA for Visual-servoing Based Underwater Vehicle

Khin Nwe Lwin, Kenta Yonemori, Myo Myint, Mukada Naoki

Mamoru Minami, Akira Yanou and Takayuki Matsuno

Graduate School of Natural Science and Technology

Okayama university

Okayama 700-8530, Japan

Kawasaki College of Allied Health Professions,

Department of Radiological Technology

Email: pdoj8yez@s.okayama-u.ac.jp

Email: minami-m@cc.okayama-u.ac.jp

**Abstract**—Genetic algorithm (GA) has been applied for real-time pose estimation in this research because of its simplicity, global perspective and repeatable ability. In many of these different situations or problems, optimum selection parameters are a critical factors in the performance of GA. We have developed visual-servo type underwater vehicle using dual-eye camera and 3D marker using real-time pose tracking, named as Real-time Multi-step GA. The relative pose between a vehicle and a 3D-marker can be estimated by Model-based matching method. To recognize the pose of the marker with respect to the vehicle, it is needed to utilize the optimum searching in real-time, and the real-time pose estimation problem can be converted into an optimization problem over a time-varying distribution function with multiple variables. Therefore, analyses the convergence performance of real-time multi-step GA for 3D model-based recognition for underwater vehicle was conducted and reported in this paper. The main aim of this paper is to choose the best parameters for GA that are optimized over population size, selection rate, mutation rate based on their relative fitness value to improve the performance of searching in time domain. The experimental results show that the proposed system effectively improved the searching performance of Real-time multi-step GA for real time pose tracking, having enable an automatic docking of underwater vehicle by dual-eyes visual servoing.

**Keywords:** Real-time Multi-step GA, Visual-servoing, Performance analysis, Underwater vehicle

## I. INTRODUCTION

GA is an evolutionary algorithm for searching and optimization based on natural selection and natural change of generation. It have been applied to a wide range of complex problems in numerous areas of science, engineering and etc. Genetic algorithms (GAs) are generally able to find optimal solutions of hard problem in reasonable amounts of time. But when GA is applied to complex and difficult problems, it needs an increase in the time required to find good solutions. Since GA only needed the way to evaluate the performance of its solution then it can be applied generally to any optimization problem without assumptions.

Optimization problems are used to find the optimal solution based on the evaluation function of the system. There are many

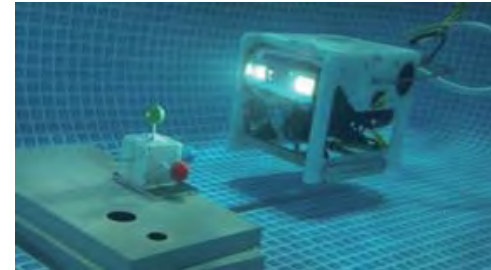


Fig. 1. Underwater Vehicle and 3D Marker

typical optimization techniques such as linear programming, iterations, simple heuristic functions, depth first search and breadth first search. To the best author knowledge, there is few related works in which advanced optimization techniques are applied in applications where real time performance is dominant.

In today world, visual servo based underwater vehicles have being conducted for many purposes such as inspection, repair oil and gas, docking task, scientific studies of the deep ocean, etc. The task of visual servoing is to use the feedback information to control the position and orientation of the robot with respect to a target object. The studies on visual servoing based underwater vehicle have been conducted all over the world in recent year. Almost studies are based on single eye camera to estimate the pose of the target object[1][2]. However, the visual servoing performance using single camera is often gauged inaccurately especially in term of 3D depth information. To solve this problem, visual servo type underwater vehicle using dual-eye camera and 3D marker has been developed using real-time pose tracking by means of visual servoing as shown in Fig.1. To the best of author's knowledge, visual servoing using stereo vision with two cameras is initiated by our group research. The vehicle's pose with respect to the target is estimated in real-time by using model-based matching and real-time multi-step genetic algorithm. To recognize the pose of the target object with respect to the vehicle, it is needed to utilize optimum searching for real-time.

The proposed system is performed by applying the real-time multi-step GA for optimization problem of searching for the optimum solution. Conventional GA has been proved that it is useful for many optimization problems but they have limitation especially in time domain. Instead of getting the best accuracy with limitation for real-time application, an approach that is simple, be able to converge for real-time performance with repeatable ability is considered in proposed system. However, the configuration of GA effects the recognition performance. Therefore, performance analysis of GA for real-time 3D model-based recognition for underwater vehicle was conducted and reported in this paper. There are many researches related to the analysis of GA performance based on modification of GA parameter [3]-[8]. Even though there are many powerful optimization methods, Genetic algorithm is used in this experiment because of its simplicity, repeatable ability and especially effectiveness in real-time performance. The main aim of this paper is to analyse the parameters value of GA that generate the best population size, selection rate and mutation rate that improve the performance of searching for real time operation. Finally, we confirmed that the proposed system could perform the real-time recognition performance using the best GA parameters experimentally.

## II. PROPOSED SYSTEM

### A. 3D Model-based Matching Method with Stereo Vision System

Visual servoing is used to control of robot motion by utilizing feedback information from vision sensor that is mounted on the vehicle. In this experiment, the pose (position and orientation) of the robot relative to the target object is estimated by applying 3D model-based matching method and dual-eyes camera. In proposed system, applying dual-eyes cameras can support better performance than using one camera. 3D Model-based pose estimation using dual-eyes vision system is shown in Fig.2.  $\Sigma_{CR}$  and  $\Sigma_{CL}$  are the reference frames of dual-eye camera which are mounted in front of the vehicle.  $\Sigma_H$  is reference frame of the ROV. The search space of the vision system is already defined as can be seen in Fig.4. 3D marker which is composed of three spheres whose color are red, green and blue is used as a target object. There are many models located in search area with different poses. The solid model of the marker is the captured 2D image by dual-eye camera and the dotted-line model is the projected image from 3D to 2D image. The different relative pose between the vehicle and the target object is calculated by comparing the projected 2D image and the solid object image captured by dual-eye camera. Finally, the best model that represents truthful pose can be obtained based on its highest the fitness value of each model.

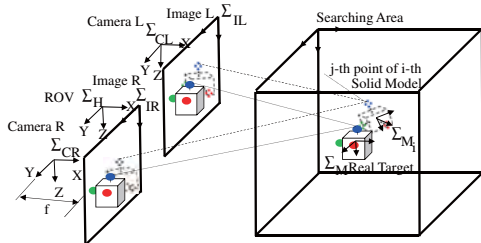


Fig. 2. 3D Model-based Matching Method with Stereo Vision System

## III. GENETIC ALGORITHM

Genetic algorithm is utilized to solve searching problem by means of optimization one. Firstly, Genetic algorithm generates random population of GA individual candidates, where strings of bits are used to represent the candidate as chromosomes. A population comprises a set of chromosome that contained of genes candidate. Every gene of chromosome is expressed as the two possible values 0 and 1. Each individual candidate get its pose information by evaluating using fitness function shown in equation (3) based on the maximum fitness value. This evolution process carried out the maximum fitness value of each generation of every individual model to form the next generation. At this time, the set of generation have fitter position and orientation with good fitness value than the previous generations, that is closer toward the maximum value near the fitness function that represents the object. These possible models reproduce new generations by selection and recombination method which represents a better solution to the real target pose estimation. Then again new generations are formed from mutation or crossover operations of GA. By performing this process repeatedly, GA searched the optimum value that indicates the pose of the object relative to the vehicle. Initial population of GA is generated in random and GA candidates are evaluated by the operators; selection, crossover and mutation.

### A. Selection Operator

The selection operator selects the chromosome from the current generation based on fitness value and chooses the better chromosome to reproduce the next generation. The fitness function execution is dependent on the specify as a condition. The fitness function supported the GA to analyse the performance of each chromosome in the population. There are different types of selection process such as Roulette-Wheel selection, Ranking-based selection, Tournament selection and Elitism. In this paper, the process of ranking based selection is considered. Generally, if the maximum fitness value of number of chromosomes are increased the probability of selection rate will increase. It will not be possible that the optimum solution is obtained by running the GA in one time. But, the probability of selection operator will converge to the real solution, if the GA is run repeatedly.

### B. Crossover Operator

The crossover operator generates and creates the new chromosome from the current string. The performance of crossover operator is to exchange the position between the strings randomly. There are many ways to be chosen more crossover points such as two-point crossover and multi-point crossover. For the specific problem, it is needed to determine specific crossover so that the performance of GA can be improved. Two point crossover is used in this experiment.

### C. Mutation Operator

After the crossover had performed the mutation will operate. This operator randomly changes one or some bits in the result from crossover process within the population.

#### D. Real-time Multi-step GA

Real-time multi-step GA is used for searching problem of pose recognition based on time domain. It means that the real-time multi-step GA can evaluate the optimum solution by the sampling rate (video rate) of 33 [ms] in the experiment. The pose of the individual represents by six parameters in the population. The upper 36 bits (12 bits for each x, y, z) represents the position coordinate of the three dimensional model of the gene. The remaining 36 bits (12 bits for each  $\epsilon_1, \epsilon_2, \epsilon_3$ ) describes the orientation defined by quaternion. Therefore, the sufficient evolution time and population size will be analysed in the next section. Fig.3 represents the flowchart of real-time multi-step GA and Fig.4 shows the GA searching area.

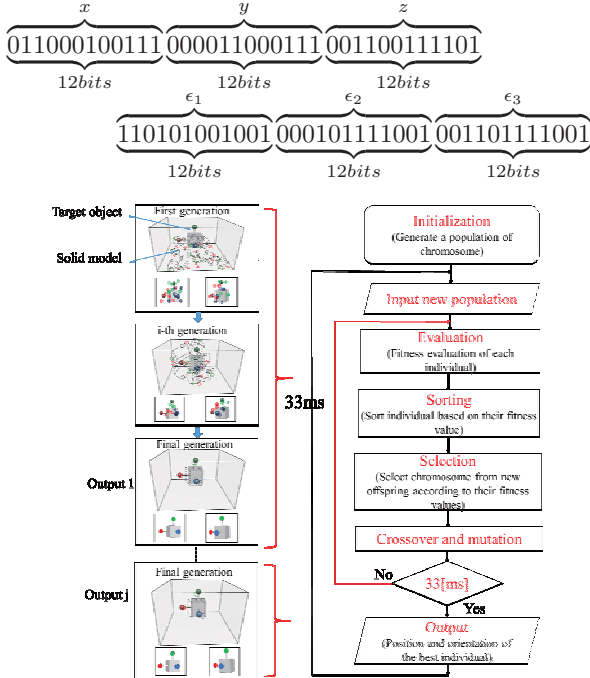


Fig. 3. Flowchart of Real-time Multi-step GA

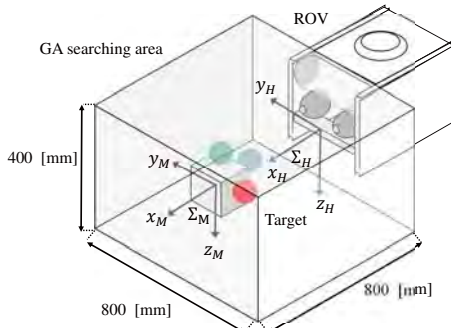


Fig. 4. GA Search Area

## IV. ANALYSIS AND DISCUSSION OF RESULTS

#### A. Experimental setup

Figure.5 shows the experimental tank which is an indoor pool (length 750[mm] × width 570[mm] × height 490[mm]).

filled with water and the distance between the vehicle and static 3D marker was 350[mm]. ROV received the dynamic image information through the cable connected to PC. In this experiment, not only dynamic images but also static images are used to analyse performance of real-time multi-step GA. The next section will discussed on experiment and results in detail.

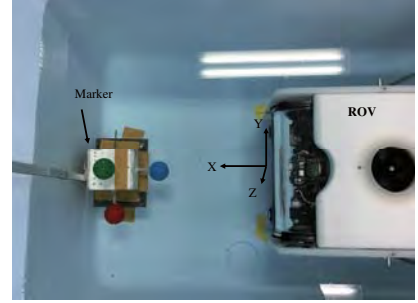


Fig. 5. Experiment Layout

#### B. Fitness Function

The poses of the 3D-marker could not be recognized directly by image features in model-base matching method. But the optimal solution can be obtained based on the fitness value of each model of the target by searching with genetic algorithm. Fig.6 shows the real target and model of 3D marker. In this system, only hue value is used for recognition of 3D marker because of less sensitive to environment. In each ball in each model consists of two portions, the first portion is the inner area which is the same size with the target and the second portion is the background area. The capture image (pixel) is detected in 2D image as (green or blue or red) in hue space. If the capture image(pixel) situated in inner portion the fitness value will be increased and the capture image (pixel) is situated in outer portion, the fitness value will be decreased. Therefore, the fitness value will be maximum when the model and the real target are identical. Finally, the averaged fitness value of the dual-eyes cameras is calculated as the following equations (1-3). Detailed explanation about GA method and fitness function is referred to our previous paper [11].

$$F_R(\varphi) = \frac{1}{\wedge} \sum_{k=1}^m \left( \sum_{IR_{ri} \in S_{R,in,k}(\varphi)} \delta(h(IR_{ri}) - b_k) \right) - \sum_{IR_{ri} \in S_{R,out,k}(\varphi)} \delta(h(IR_{ri}) - b_k) \quad (1)$$

$$F_L(\varphi) = \frac{1}{\wedge} \sum_{k=1}^m \left( \sum_{IL_{ri} \in S_{L,in,k}(\varphi)} \delta(h(IL_{ri}) - b_k) \right) - \sum_{IL_{ri} \in S_{L,out,k}(\varphi)} \delta(h(IL_{ri}) - b_k) \quad (2)$$

$$F(\varphi) = (F_R(\varphi) + F_L(\varphi))/2 \quad (3)$$

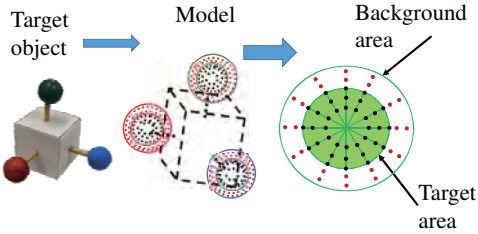


Fig. 6. Real Target and Model of 3D-marker

TABLE I. SETTING PARAMETER OF GA

Population	40	60	80
Selection rate [%]	20, 40, 60	20, 40, 60	20, 40, 60
Mutation rate [%]	5, 1, 15	5, 1, 15	5, 1, 15
Crossover	Two point		
Number of Evolution[times/33ms]	9		

### C. Choosing of Selection Rate and Mutation Rate

Our experiment was conducted using 60% elitism, two points crossover, 1% mutation. We began with instance population size of 40, 60 and 80. Firstly, the recognition accuracy was analysed based on different population size (40, 60, 80), selection rate (0.2, 0.4, 0.6) and mutation rate (0.5, 1, 1.5). TableI shows the setting parameters for analysing of GA performance. In this experiment, ranking based selection, two points crossover and termination in 33 [ms] were considered. According to the experimental results selection rate 0.6 and mutation rate 0.1 are selected.

### D. Choosing of Population Size

Genetic parameters namely as selection, crossover, mutation and population size are key factor to obtain the optimum accuracy of the system, these parameters are considered as primarily parameters. Fig.7 shows the analysis of evolution times based on different population size from 10 to 500. Firstly, we analysed how many evolution time will be generated within 33 [ms] based on different number of population sizes. The evolution times within 33 [ms] (video rate) is inversely proportional to the number of population size. In this case, we have to choose the optimum number of population size with reasonable number of evolution time for real-time performance. Based on the experimental result of evolution times data, we analysed the convergence performance of real-time multi-step GA by using dynamic images and static images as can be seen in Fig.8 and Fig.9.

In Fig.8, graph shows that the time response of the convergence performance has been achieved for all population size but not the same quick response time of the fitness value. The population size at the end of evolution time within 33 [ms] (based on different evolution time) from best to worst is 40, 60, 80, 100, 200, 300, 400, 500. Even though the fitness value of the different number of population sizes are maintained above 0.8 the quick response time of population size 40 is faster than other population sizes. In this experiment, the fitness value needed to have the value of 0.5 or more for good performance of GA recognition accuracy. Fig.9 shows the result of real-time GA convergence performance using static images. In this figure, the convergence performance of eight population sizes with different fitness values have been obtained. It is clear that

TABLE II. BEST PARAMETERS FOR GA

Number of genes	40
Search area [mm]	$[x, y, z] = \pm 400 \pm 200 \pm 400$
Selection probability	0.6%
Mutation probability	0.1%
Number of Evolution	14
Control Period [ms]	33
Target variable	Position (x[mm])

the determination of population size is importance for real-time recognition accuracy based on the evolution times. The quick response time of the population size (100, 200, 300, 400 and 500) gradually increase until 0.8 and the stabilization was occurred after 0.8 seconds. Population size 40, 60 and 80 will converge quickly within a few seconds. However, population size 40 is the best population size for the real-time performance according to the experimental result by using static and dynamic images.

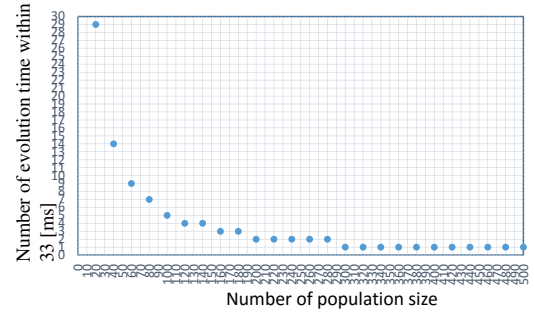


Fig. 7. Evolution Time of GA

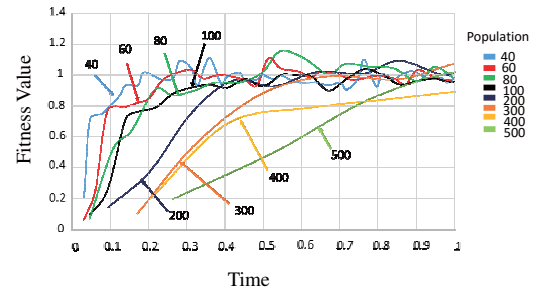


Fig. 8. Convergence Performance of GA with Dynamic Image

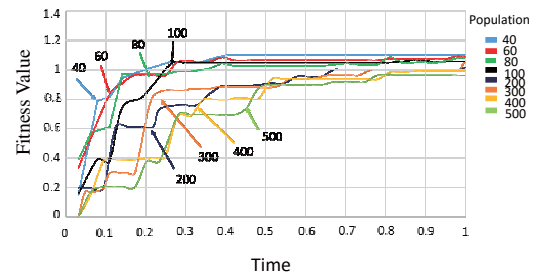


Fig. 9. Convergence Performance of GA with Static Image

### E. Comparison of GA Search and Full Search using Off-line Adaptation

We evaluated the recognition accuracy by using full search multi-step GA. Fig.10 shows the recognition comparison of position Y-Z plane between the GA search and the full search process. The full search is a method to evaluate the result of real-time multi-step GA by analysing the specific image where real-time multi-step GA get the corresponding fitness value. The main idea of full search is to calculate the fitness of every points which are 1[mm] apart in the entire searching area. By using GA search process, the recognition accuracy of maximum fitness value is (1.213) and the position is 14.0625 [mm] in Y plane and -72.3711 [mm] in Z-plane. In full search process, the maximum fitness value is (1.3611) and the position of (Y,Z) plane are 15 [mm] and -72 [mm] respectively. It is obvious that the small error will be occur in (y,z) plane about 0.9[mm] and -0.3711[mm]. Finally, we obtained the best GA parameters for the real-time recognition performance as shown in Table.II.

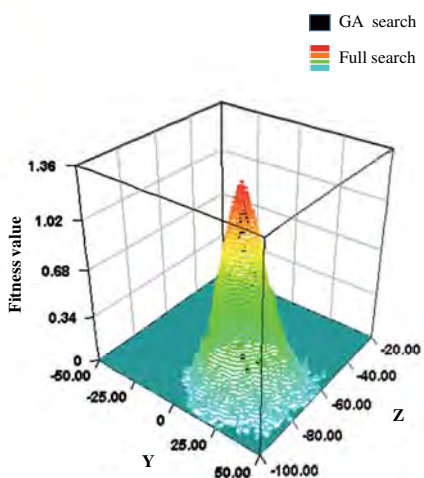


Fig. 10. Full search and GA search

## V. DOCKING PERFORMANCE USING THE BEST GA PARAMETER

Finally, We conducted the repeated docking experiment in indoor pool to verify whether the the proposed system can operate the real-time performance using the best GA parameter.

### A. Structure of Docking Station

Docking station was designed as shown in Fig.11. The target object and the docking hole is fixed in docking station. The diameter of the docking hole is 70 [mm] and the center distance between the marker and the docking hole is 160 [mm]. The structure of docking experiment and the three underwater cameras are mounted as shown in Fig. 11.

### B. Experiment Environment

The ROV was designed and fabricated by KOWA cooperation as shown in Fig.5. In this robot system, the eye visual sensor is used as a main sensor. There are totally four cameras (imaging element CCD, 380,000 pixel, signal system NTSC,

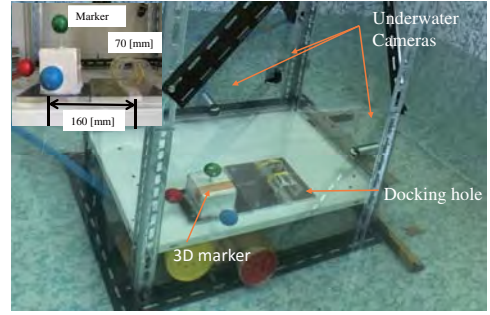


Fig. 11. Structure of Experiment Layout

Minimum Illumination 0.8[1X], without zoom) are mounted in this model and the two front cameras are used to perform a three-dimensional object recognition in visual servoing. Four thrusters are used in system, maximum thrust force is (9.8[N]) in horizontal and maximum vertical thrust force is (4.9[N]). In addition, the LED lights (5.8W) has been equipped for illumination ensure. The ROV obtains the camera image information and control signal from the PC through a tether cable (200[m]). It can operate in maximum water depth 50[m]. Then, a simple pool ( length 2870[mm] width 2010[mm] height 1000[mm])is used as an experiment tank which was filled with tap water. Fig.12 shows the layout of underwater experimental device. Power supply and transmission of the control signal from the PC is made through a tether cable (200 [m]).



Fig. 12. Underwater Experiment Environment

### C. Controller

Proportional controller is used to control the vehicle. The four thrusters that are mounted on the underwater robot are controlled by sending the command voltage based on the feedback relative pose between the underwater robot and the object ( $x_d$ [mm],  $y_d$ [mm],  $z_d$ [mm]). The block diagram of the control system is shown in Fig.13. The control voltage of the four thrusters are controlled as the following equations.

$$\text{The depth direction} : v_1 = k_{p1}(x_d - x) + 2.5 \quad (4)$$

$$\text{Vertical axis rotation} : v_2 = k_{p2}(\epsilon_{3d} - \epsilon_3) + 2.5 \quad (5)$$

$$\text{Vertical direction} : v_3 = k_{p3}(z_d - z) + 2.0 \quad (6)$$

$$\text{Horizontal direction} : v_4 = k_{p4}(y_d - y) + 2.0 \quad (7)$$

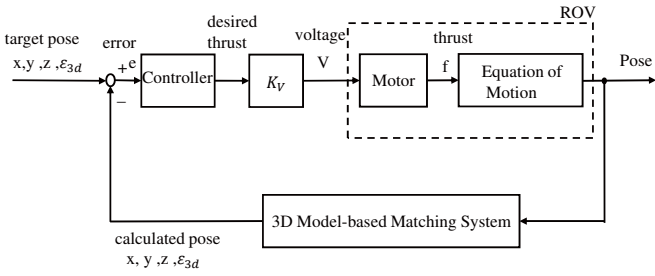


Fig. 13. Block Diagram of Visual Servo Control

Where  $v_1$ ,  $v_3$  and  $v_4$  are the control voltage of the four thrusters of x, z, y direction respectively.  $x_d$ ,  $y_d$ ,  $z_d$  are the desired relative pose between the vehicle and the target.  $\epsilon_{3d}$  is the rotation direction around the z-axis and it is expressed as the value of  $v_2$ . According to the experimental result, the gain coefficient is adjusted to perform the best condition for visual servoing.

#### D. Docking Performance

We conducted the repeated docking experiment in indoor pool. In this experiment, the desired pose ( $x_d = 600$ ,  $y_d = -10$ ,  $z_d = -10$  and  $\epsilon_{3d} = 0$ ) between the target and the ROV are predefined so that the robot will perform station keeping through visual servoing. After the docking had performed each time it will go back to the predefined distances. There are totally 27 points of predefined distance as shown in Fig.16. We can see one of the docking experiment result in Fig.14 where the starting point is 1. Fig.14 (a) shows the fitness value of GA recognition that is maintained above 0.6, it means that the real target and model are matching well. Fig.14 (b) to (e) shows the position between desired and the estimated pose of the 3D marker recognized by GA and the relative target pose. At the start condition, the visual servoing state will be occurred in x, y, z and position around in z-axis within a few minutes. In visual servoing state, the robot detect the 3D marker and relative pose with respect to the vehicle. After visual servoing had performed, the docking operation was started around at time=3[s]. In docking state, the rod is attached to the vehicle to dock into the docking hole as shown in Fig.16. When the robot is stable within desired relative error  $\pm 20$  [mm] in Y-Z plane for 165 [ms], the rod is fitted into the docking hole by decreasing the desired value of  $x_d$ . Finally, the docking operation completed successfully about 15 [s]. It can be confirmed that it is possible to regulate the surrounding region of the relative target pose. Fig.14 (g) to (J) represent the thrust to restore the error respectively. Fig.14 (f) describes the 3D trajectory for underwater vehicle during docking process. According to the experimental result from these figure, it can be confirmed that the proposed system can perform the successful docking operation.

#### E. GA Performance Analysis of Docking Experiment

Even though the top gene is searched and selected to represent truthful pose, the rest genes are analysed to check they are distributed well so that top genes can converge to the solution quickly and also other genes are diverged enough to cover the searching area. Fig.15 shows real-time multi-step GA performance analysis of docking experiment. Fig.15

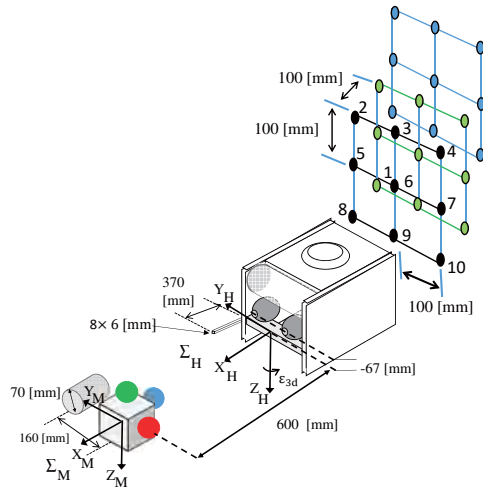


Fig. 16. Docking Coordinate and Predefined Points

(a) shows the 3D trajectory tracking during docking process. Fig.15 (b) represents the distribution of all gene value in x-axis direction. 60% of top gene in x-axis direction converged to the real solution and 40% of other genes are divergent as shown in Fig.15 (c) and (d). According to the result as shown in Fig.15 (c), it was confirmed that top gene 60% convergence to the real solution following the selection rate of 0.6. On the other hand, the bottom-gene 40% diverge enough not to miss the target when ROV moves quickly. Fig.15 (f) shows the accuracy comparison of the recognition in position Y-Z plane between the GA search and the full search process at sampled point ( $t=12.262$  [s]) while docking operation. By using GA, the recognition accuracy of maximum fitness value is (1.21) and the position is -14.9492 [mm] in Y plane and 11.3281 [mm] in Z-plane. In full search process, the maximum fitness value is (1.11) and the position of (Y,Z) plane are -14[mm] and 12 [mm] respectively. It is obvious that the small error will be occur in (y,z) plane about -0.94292[mm] and 0.6719[mm]. We can clearly see the position of each top genes from the 2D graph in Fig.15 (e). The standard deviation of recognized position in Y-axis and Z-axis direction is shown in Fig.15 (g). Therefore, it was confirmed that the selection rate 60% is convergence to the real solution.

## VI. CONCLUSION

In this study, performance analysis and optimization of real-time multi-step GA for real time recognition for underwater vehicle by using 3D marker and dual-eye camera is presented. Population sizes, selection rate and mutation rate that influences on the recognition accuracy are analysed and selected for proposed system. We confirmed and analysed the data of the repeated docking experiment by using the best GA parameter. Investigating these result, it can be concluded that the real time recognition accuracy of the system is effective. Experimental results show that the recognition accuracy of the system is optimized with the error in [mm] level for real time recognition.

## REFERENCES

- [1] George C.Karrs and Kostas J.Kyriakopoulos, "Visual servo control of an underwater vehicle using a laser vision system," *IEEE/RSJ International Conference on Intelligent Robots and Systems*, pp. 101-106, 2000.

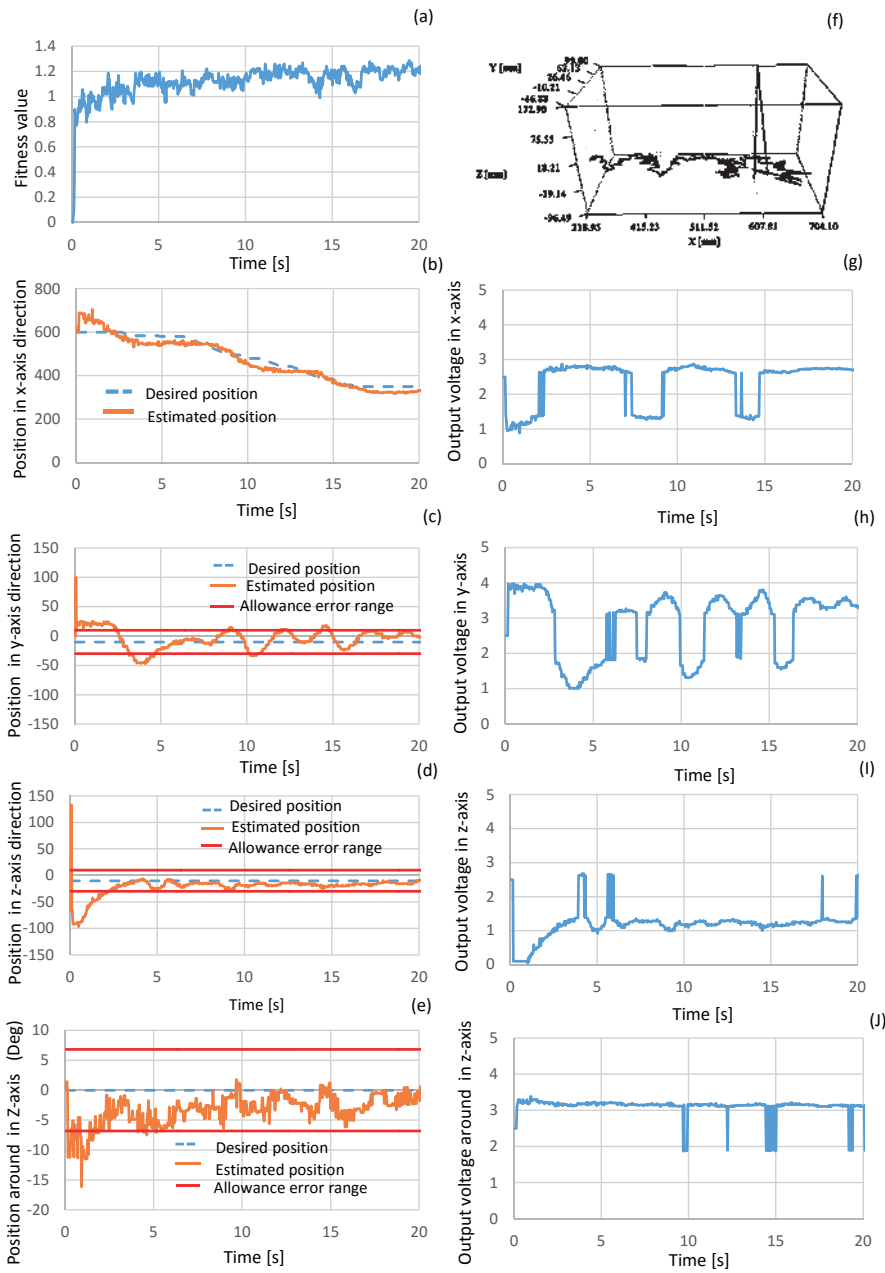


Fig. 14. Docking Performance: (a) Fitness value (b) Position in X-axis direction (c) Position in Y-axis direction (d) Position in Z-axis direction (e) Position around in Z-axis direction (f) 3D trajectory of underwater vehicle(g) Output voltage in X-axis (h) Output voltage in Y-axis (I)Output voltage in Z-axis (J)Output voltage around in Z-axis

- Conference on Intelligent Robots and Systems*, Acropolis Convention Center Nice, France, Sept, 22-26, 2008.
- [2] XunLi, Jinling Wang, Nathan Knight, Wedidong Ding, " Vision-based positioning with a single camera and 3D maps: accuracy and reliability analysis," *Journal of Global Positioning Systems*, vol. 10, no. 1:19-29, DOI:10.5081/jgps.10-1-19, 2011.
  - [3] Ignacio Rojas, Jess Gonzalez, Hector Pomares, J. J. Merelo, P. A. Castillo, and G. Romero, "Statistical analysis of the main parameters involved in the design of a genetic algorithm," *IEEE Transaction on Systems, Man, And Cybernetic-Part C: Applications and Reviews*, vol. 32, no. 1, February 2002.
  - [4] D. E. Goldberg, K. Deb, and J. H. Clark, "Genetic algorithms, noise, and the sizing of populations," *syst.*, vol. 6, pp. 333-362, 1992.

- [5] E. Eiben, R. Hinterding, and Z. Michalewicz, "Parameter Control in Evolutionary Algorithms," *IEEE Transactions on Evolutionary Computation*, vol. 3, no. 2, pp. 124-141, 1999.
- [6] J. Schaffer, R. Caruana, L. Eshelman, and R. Das, "A study of control parameters affecting online performance of genetic algorithms for function optimization," in *Proc. 3rd Int. Conf. Genetic Algorithms*, pp. 51-60, 1989.
- [7] Z. M. Jaroslaw Arabas and J. Mulawka, "GAVaPS-a genetic algorithm with varying population size," *IEEE International Conference on Evolutionary Computation*, pp. 73-78, 1995.
- [8] C. R. Reeves, "Using genetic algorithms with small populations," in *Proceedings of the 5th International Conference on Genetic Algorithms*, pp. 92-99, 1993.

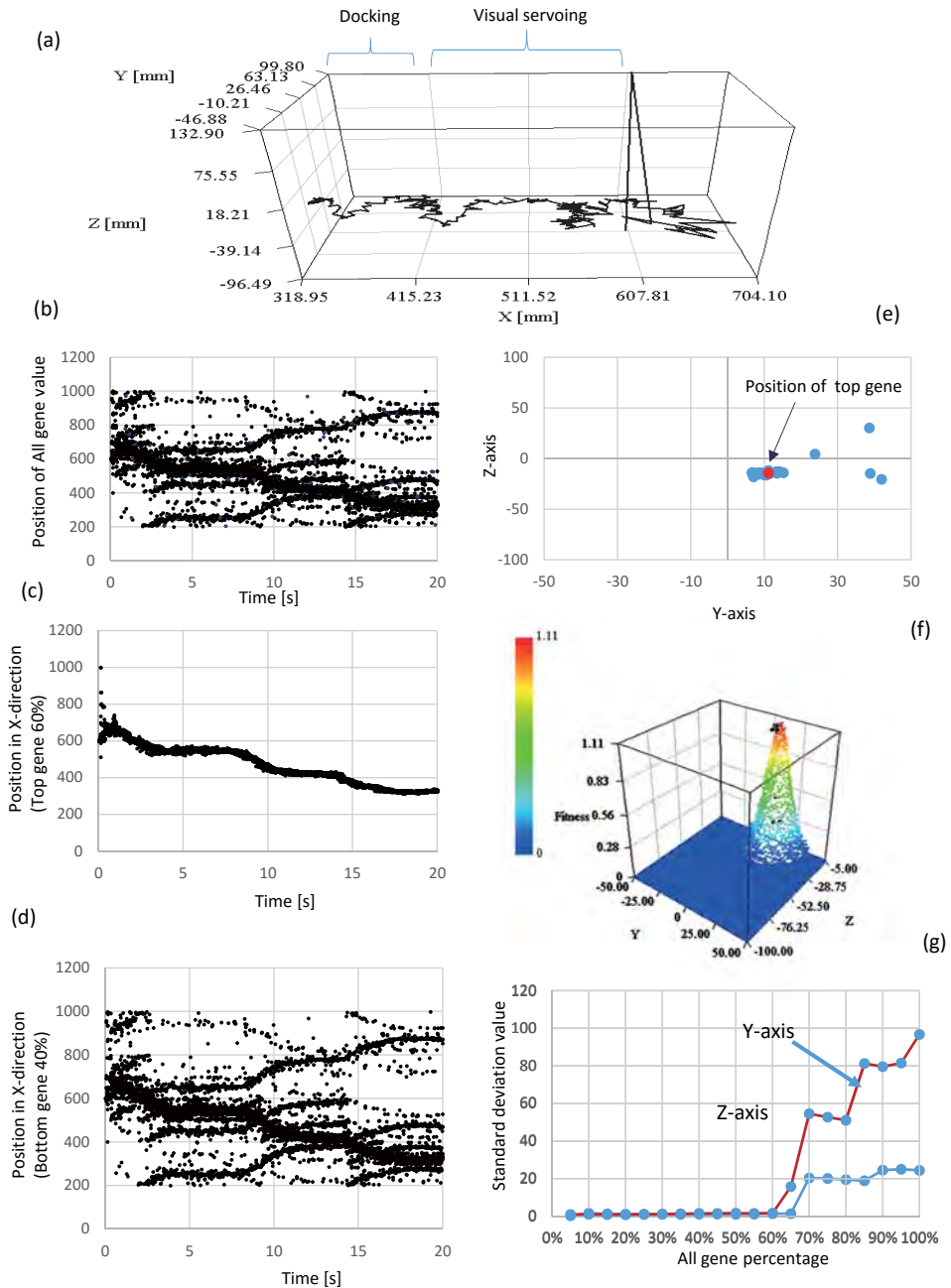


Fig. 15. All gene data analysis: (a) 3D trajectory of underwater vehicle (b) Position of all gene value (c) Position in X-direction(Top gene 60%) (d) Position in X-direction(Bottom gene 40%) (e) Position of top gene in 2D graph (f) GA search and full search (g) Standard deviation of Y-axis and Z-axis

- [9] Michalewicz Z., "Genetic algorithms+data structures=evolution programs," Second, Extended Edition, Springer-Verlag, Berlin, Heidelberg, 1994.
- [10] Myo Myint, Kenta Yonemori, Akira Yanou, Shintaro Ishiyama and Mamoru Minami, "Robustness of visual-servo against air bubble disturbance of underwater vehicle system using three-dimensional and dual-eye cameras," MTS/IEEE OCEANS 15 Washington, DC, October 19-22.
- [11] Yu F., Minami M., Song W., Zhu J. and Yanou A., "On-line head pose estimation with binocular hand-eye robot based on evolutionary model-based matching," Journal of Computer and Information Technology, vol. 2, no. 1, pp. 43-54, 2012.
- [12] Myo Myint, Kenta Yonemori, Akira Yanou, Mamoru Minami and Shintaro Ishiyama, "Visual servo-based autonomous docking system for un-

- derwater vehicle using dual-eyes camera 3D pose tracking," Proceedings of the 2015 IEEE/SICE International Symposium on System Integration, Nagoya, Japan, pp. 989-994, 2015.
- [13] Song W. and Minami M., "3-D Visual servoing using feed-forward evolutionary recognition," Journal of the Robot Society of Japan, vol. 28, no. 5, pp. 591-598 (in Japanese), 2010.
- [14] Myo Myint, Kenta Yonemori, Akira Yanou, Mamoru Minami and Shintaro Ishiyama, "Visual-based autonomous underwater vehicle docking system using stereo vision," IEEE Journal of Oceans Engineering, 2016.